

Article

Derivation of Landslide Rainfall Thresholds by Geostatistical Methods in Southwest China

Zhongyuan Xu ^{1,2} , Zhilin Xiao ^{1,*}, Xiaoyan Zhao ², Zhigang Ma ¹, Qun Zhang ¹, Pu Zeng ³ and Xiaoqiong Zhang ³

¹ Sichuan Institute of Land and Space Ecological Restoration and Geological Hazard Prevention, Chengdu 610036, China; zyxu@swjtu.edu.cn (Z.X.); xfy_mzg@163.com (Z.M.); zq_sxfy@163.com (Q.Z.)

² Faculty of Geosciences and Engineering, Southwest Jiaotong University, Chengdu 611756, China; xyzhao2@swjtu.edu.cn

³ Natural Resources and Planning Bureau of Ya'an City, Ya'an 625099, China; wangyishouye@yeah.net (P.Z.); zhangxq_yaan@yeah.net (X.Z.)

* Correspondence: xfyxzl@163.com

Abstract: Deriving rainfall thresholds is one of the most convenient and effective empirical methods for formulating landslide warnings. The previous rainfall threshold models only considered the threshold values for areas with landslide data. This study focuses on obtaining a threshold for each single landslide via the geostatistical interpolation of historical landslide–rainfall data. We collect the occurrence times and locations of landslides, along with the hourly rainfall data, for Dazhou. We integrate the short-term and long-term rainfall data preceding the landslide occurrences, categorizing them into four groups for analysis: 1 h–7 days (H1–7), 12 h–7 days (H12–D7), 24 h–7 days (H24–D7), and 72 h–7 days (H72–D7). Then, we construct a rainfall threshold distribution map based on the 2014–2020 data by means of Kriging interpolation. This process involves applying different splitting coefficients to distinguish the landslides triggered by short-term versus long-term rainfall. Subsequently, we validate these thresholds and splitting coefficients using the dataset for 2021. The results show that the best splitting coefficients for H1–D7, H12–D7, H24–D7, and H72–D7 are around 0.19, 0.52, 0.55, and 0.80, respectively. The accuracy of the predictions increases with the duration of the short-term rainfall, from 48% for H1–D7 to 67% for H72–D7. The performance of these threshold models indicates their potential for practical application in the sustainable development of geo-hazard prevention. Finally, we discuss the reliability and applicability of this method by considering various factors, including the influence of the interpolation techniques, data quality, weather forecast, and human activities.

Keywords: rainfall threshold; landslide warning; geostatistical interpolation



Citation: Xu, Z.; Xiao, Z.; Zhao, X.; Ma, Z.; Zhang, Q.; Zeng, P.; Zhang, X. Derivation of Landslide Rainfall Thresholds by Geostatistical Methods in Southwest China. *Sustainability* **2024**, *16*, 4044. <https://doi.org/10.3390/su16104044>

Academic Editors: Lucio Di Matteo and Michalis Diakakis

Received: 8 February 2024

Revised: 2 May 2024

Accepted: 9 May 2024

Published: 12 May 2024



Copyright: © 2024 by the authors. Licensee MDPI, Basel, Switzerland. This article is an open access article distributed under the terms and conditions of the Creative Commons Attribution (CC BY) license (<https://creativecommons.org/licenses/by/4.0/>).

1. Introduction

Rainfall is a recognized trigger for landslides and has been studied extensively due to its impact on the soil mechanics [1,2]. The infiltration of rainwater into the soil increases the pore water pressure, which can decrease the stability of slopes and trigger landslides. Additionally, rainfall can reduce the matric suction, which is the tendency of water to adhere to soil particles. This reduction in the matric suction further weakens the soil, making it more prone to landslides [3]. Weather forecasts can predict potential rainfall values several days in advance for areas that are susceptible to landslides, which can indicate the possibility of landslide activity. As a result, rainfall thresholds have become one of the most cost-effective tools in landslide warning systems and susceptibility analysis, which have been widely implemented in many regions [4–7]. The establishment of rainfall thresholds is intricately linked to the sustainable development of regional geo-hazard warning and prevention.

The concept of a rainfall threshold refers to a critical level of precipitation that, if reached or exceeded, is likely to trigger landslides [8]. There are two approaches to defining

rainfall thresholds: the physical approach and the empirical approach. The physical approach involves the consideration of the physical processes governing landslide initiation. This method can be used to determine the amount of precipitation that triggers a landslide by simulating the hydrogeological processes and material movement [9,10]. However, this approach requires a deep understanding of the hydrogeological, geomorphological, soil mechanics, and lithological conditions of the landslide, which are usually unavailable on a regional scale. Therefore, the physical approach can only be applied to very small sites [11]. In contrast, the empirical or statistical approach relies on the analysis of historical landslide events and their corresponding rainfall conditions. On the larger regional scale, this method has been widely used with functional empirical correlations between the rainfall values and landslide occurrence. The thresholds are often obtained by drawing lower-bound lines on the correlation map between two rainfall conditions. In general, four types of correlations have been commonly employed to characterize the rainfall thresholds: (i) the rainfall intensity–duration (I–D) correlation [12–14]; (ii) the short-term precipitation and antecedent effective rainfall [15,16]; (iii) the cumulated precipitation and rainfall duration (E–D) [17,18]; and (iv) the cumulated precipitation and average rainfall intensity [4,19]. In most cases, multiple lines representing the different levels of the warning system were obtained for better management [20,21]. Simple mathematical equations were used to describe these lines and predict the future possibilities of landslide occurrence.

Empirical thresholds can be applied to study areas of different scales, ranging from a few thousand square kilometers to the global scale [22]. Researchers have endeavored to establish global thresholds by scrutinizing comprehensive global landslide data [23,24]. While these global thresholds can serve as a reference for studying and forecasting landslides in the absence of local data, local thresholds are more valuable in landslide warning systems. This is because local thresholds implicitly consider the local climate conditions and local geological and geomorphological settings [8], providing a more precise prediction process. Therefore, the empirical thresholds are usually obtained after determining the geo-hazard susceptibility zones [6,25,26]. From information on landslides and high-resolution rainfall records, we are able to choose the right parameters in defining the thresholds for landslides [27,28].

Traditional threshold analysis results in great uncertainty regarding landslide occurrence predictions. The accuracy of both the I–D and E–D models depends on multiple factors, each carrying its own weight in terms of influencing the outcomes, such as the resolution of rainfall and geo-hazard data [29], the relative locations of nearby rain gauges and landslides [30], and the criterion used to define the lower bound of the threshold. To enhance the prediction accuracy of the rainfall thresholds with regard to landslide occurrence, more advanced monitoring techniques and more complex statistical models were developed in the last decade, including the utilization of higher-resolution rainfall and geospatial data [5,31], the integration of landslide-related hydrologic models [32,33], the incorporation of detailed geologic and geomorphological information on the study area [34,35], the utilization of black box models for predictive analytics [36,37], and the use of non-triggering rainfall data in the analysis [38]. These methods expanded the possibilities in the field of landslide prediction, providing a more comprehensive understanding of the landslide dynamics.

A challenge persists in accurately discerning whether a landslide is triggered by short-term or long-term rainfall within the empirical approach [39]. Generally speaking, shallow landslides and slope debris flow are usually triggered by short-term and intense rainfall, and relatively deeper landslides are more likely to occur during prolonged and sustained rainfall events [40,41]. However, the prior research has been deficient in presenting a quantitative methodology to differentiate these types [21,42,43]. This determination depends on a comprehensive understanding of the geological and geomorphological settings of landslides. Unfortunately, the detailed information necessary for each individual landslide is often elusive and unavailable in regional studies.

Previous studies have shown that the rainfall thresholds mostly define the likelihood of landslide occurrence based on empirical evidence, and these thresholds are usually determined for a particular region [6,16,22]. However, such thresholds may make it difficult to predict and prevent specific landslides. Determining the rainfall threshold for individual landslides through a straightforward statistical method and quantitatively differentiating between the landslides triggered by long-term and short-term rainfall remain two challenges in threshold model research. This study aims to calculate the rainfall thresholds for individual landslides using geostatistical interpolation, a method proven to be effective for this purpose [35]. Additionally, we quantitatively classify the landslides into short-term and long-term rainfall triggering events by defining and applying a splitting coefficient. Our findings demonstrate that geostatistical interpolation is a valuable tool in predicting the likelihood of landslide occurrence.

2. Materials and Methods

2.1. Study Process

In this method, rainfall data and information on landslides that had occurred were collected and extracted from the study area. We considered four types of short-term rainfall conditions and one long-term rainfall condition. Subsequently, we classified the data into four categories based on the rainfall that induced landslides. Utilizing different methods of data segmentation, we generated Kriging maps to represent the distributions of short-term and long-term rainfall, using data collected from 2014 to 2020. The best rainfall Kriging maps for each of the four categories were determined through validation with data from 2021. Figure 1 shows a flowchart of this study’s methodology.

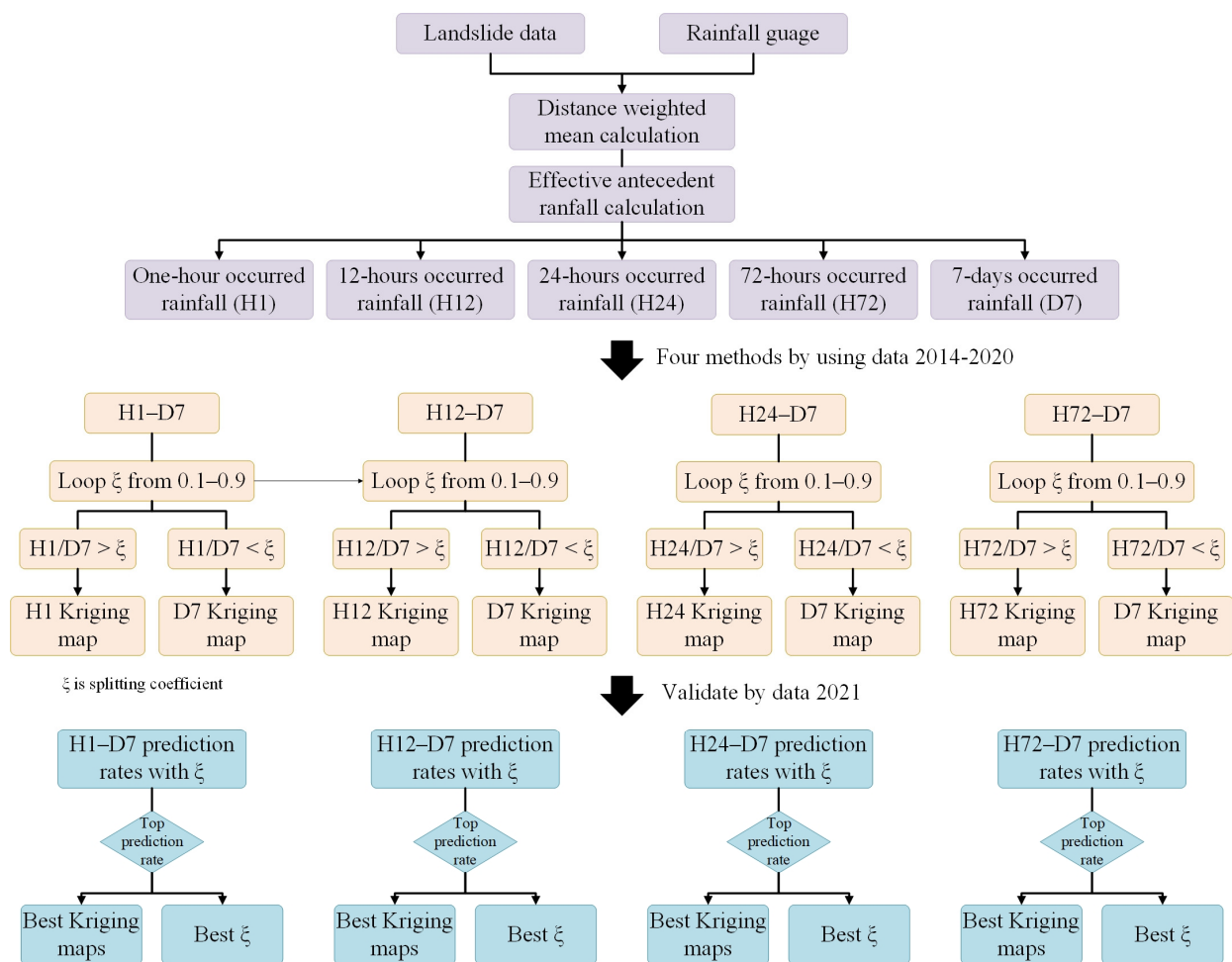


Figure 1. Flowchart of this study.

2.2. Study Area and Data Collection

Dazhou is situated in the northeast of Sichuan Province, in southwest China, with a total area of 16,591 km² and a total population of 5.4 million. The elevation increases from 200 m in the south to 2400 m in the north (Figure 2a). The northern part of Dazhou is a mountainous area, where the elevation difference usually exceeds 1000 m. The middle part is dominated by tablelands, hills, and river valleys, with the average elevation varying from 500 to 1500 m. The southern part contains alluvial flatlands split by several mountains and hills. Generally, the study site is primarily occupied by mountain landforms, which account for 70.7% of the total area, while hills account for 28.1%, and flatlands only account for 1.2% [16,44]. The general climate is humid and monsoonal, with a mean annual temperature of 14.7–17.6 °C, and the major vegetation is subtropical evergreen broadleaf forests [45]. The average annual precipitation is 650 to 1350 mm, with the north being wetter than the south (Figure 2b). Most regions have an annual precipitation level of more than 900 mm, providing favorable rainfall conditions for landslide occurrence. Dazhou is surrounded by the Daba Mountain Region and East Sichuan arc-like fold belts, which have developed a large amount of fractures and folds. The stratum lithology is mainly of mudstone, shale, sandstone, and limestone, formed in the Triassic, Jurassic, or Cretaceous periods [46].

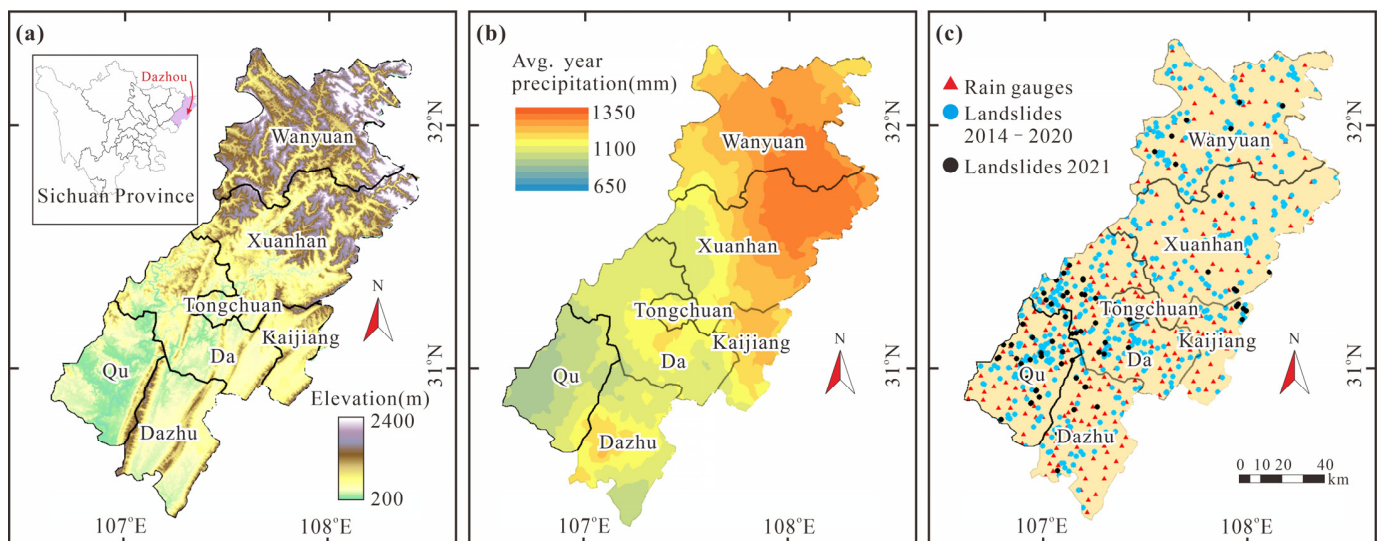


Figure 2. The elevation, climatic, and landslide information for Dazhou: (a) elevation; (b) average annual precipitation; (c) rain gauges and landslides.

Landslides are the major geo-hazard in Dazhou. From 2014 to 2021, landslide disasters caused about USD 107 million in economic losses, and the affected population exceeded 2700. The validated landslide data used in this study were collected from two government departments: (1) the Sichuan Institute of Land and Space Ecological Restoration and Geological Hazard Prevention and (2) the Natural Resources and Planning Bureau of Ya'an City. These data were recorded by geo-hazard surveyors and included the landslide triggering factors, the longitude and latitude, the time of occurrence, a description of the on-site situation, the landslide volume, the number of victims, the economic losses, etc. Rainfall data for 2014 to 2021 were provided by Sichuan Provincial Meteorological Service. The database contains a total of 532 landslides, providing information on their occurrence time, location, and scale and the damage they induced. After excluding 18 large and deep landslides and 29 landslides triggered by external factors such as human construction activities (25 landslides) and earthquakes (4 landslides), we selected 485 shallow landslides, which are labelled as rainfall-induced. Of these, nearly 90% (431 landslides) are small landslides (volume < 1×10^5 m³) and others are medium (volume $1 \times 10^5 \sim 1 \times 10^6$ m³); the lithology type of over 70% (354 landslides) consists of sandstone and mudstone, 12%

(57 landslides) are carbonate rock, and the remaining few are composed of various other lithological types. Additionally, only 78 landslide data were recorded at the exact time of occurrence in the day; for other landslides, the dates of their occurrence were recorded (Figure S1). Furthermore, the database included hourly precipitation data collected from 312 rainfall gauges. The locations of the landslides and rainfall gauges are shown in Figure 2c, and the relationship between the two datasets is displayed in Figure 3. Generally, the amount of precipitation is positively correlated with the number of landslides. The monsoon season (June–September) accumulates a high proportion of rainfall, and nearly all landslides (88%) were triggered during this period (Figure 3a), particularly in July and August. From 2014 to 2021, there was no apparent relationship between the annual precipitation and the number of landslides (Figure 3b). More landslides were recorded from 2019 to 2021, but this is likely due to the increasing attention paid to geo-hazards in recent years.

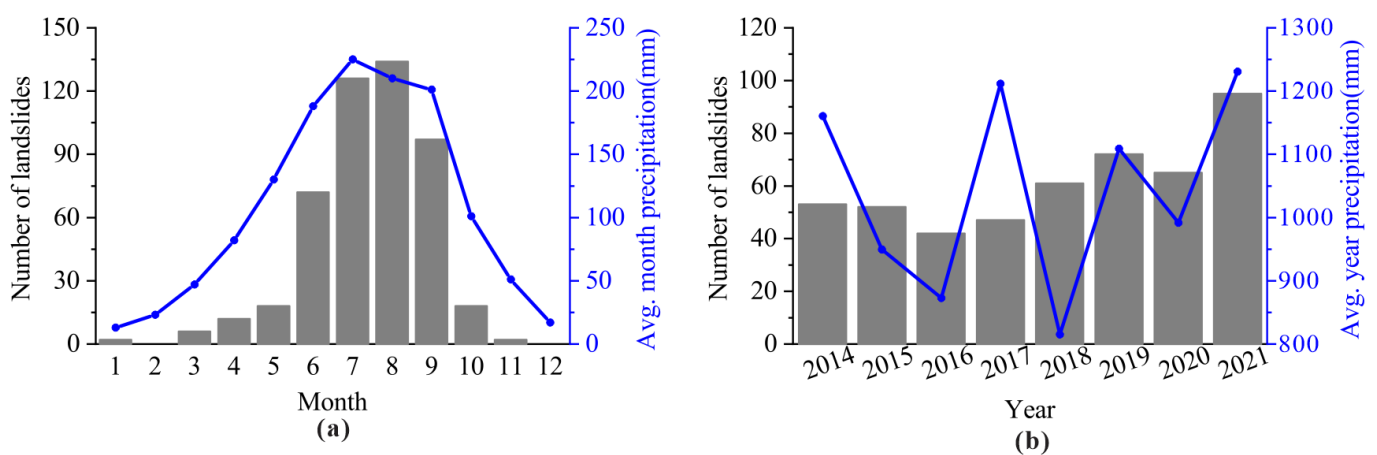


Figure 3. The relationship between the number of landslides and the amount of precipitation: (a) number of landslides each month; (b) number of landslides each year.

2.3. Rainfall Parameters of Landslides

We calculated the rainfall parameters of each landslide based on the data from the relevant rain gauges. However, there is currently no consensus on how to select the most appropriate rain gauges for landslides [11,23]. In a methodology similar to that employed in previous studies [5,47], we computed the rainfall data from the nearest rain gauges. The rainfall parameters for each landslide were determined through the distance-weighted mean of precipitation data collected from the five nearest rain gauges (see Equation (1)). We further defined those landslides with very low rainfall (<10 mm) in the 7 days prior as being not triggered by rainfall. As a result, 68 landslides were excluded from our database during this screening process. Finally, 417 landslides with rainfall parameters in the 7 days prior to their occurrence were used in the following analysis.

$$R_h = \frac{\sum_{i=1}^n W_i R_i}{\sum_{i=1}^n W_i}, W_i = \frac{1}{D_i + 0.5} \quad (1)$$

Here, R_h is the rainfall value of a landslide; R_i is the rainfall data from the i th rain gauge; D_i is the distance between the landslide and the i th rain gauge; W_i is the weight calculated from D_i .

Rainfall infiltrates into rock and soil, which then transfers to groundwater, ultimately changing the soil moisture content. This, in turn, increases the sliding force and softens the mechanical strength of the slope. This process can take several days and can result in a landslide failure. Thus, the antecedent rainfall is a critical parameter in defining the threshold for such an event. The amount of groundwater preserved in the rock and soil

declines due to evapotranspiration and discharge processes. Therefore, instead of the accumulated antecedent rainfall, the effective antecedent rainfall (P_e) was used [48]:

$$P_e = \sum_{i=1}^n k^i P_i \quad (2)$$

where i is the number of days prior to landslide occurrence; P_i is the daily rainfall measured the i th day prior to landslide occurrence; n is the number of days considered; k is the decay factor; and k^i denotes k to the power of i . We considered $k = 0.84$ as the same value was used in previous studies on Sichuan Province [15,49].

Landslide failures are often caused by one of two rainfall situations: long-duration rainfall with a low intensity or short-duration rainfall with a high intensity [50]. Therefore, we considered a long-term parameter as well as several short-term rainfall parameters. In this study, we mainly focused on the rainfall conditions that occurred up to seven days prior to a landslide event. From statistical analyses [16] and field experiments [51] conducted in the west of China, it has been established that seven days is a reasonable period to consider the influence of antecedent rainfall on landslide development. Therefore, we chose the seven-day effective rainfall (D7) as the long-term rainfall parameter. The short-term rainfall parameters were the one-hour rainfall (H1), twelve-hour rainfall (H12), one-day or intraday rainfall (H24), and three-day effective rainfall (H72) prior to the occurrence of a landslide. Since most landslide data lack the exact time of the landslide event on the occurrence day, we considered the largest one-hour rainfall and the largest rainfall in twelve consecutive hours as H1 and H12, respectively. H24, H72, and D7 were calculated using Equation (1). Furthermore, we defined the splitting coefficient as the criterion for distinguishing short-term rainfall-triggered landslides and long-term rainfall-triggered landslides. If the ratio of short-term rainfall to long-term rainfall is larger than the splitting coefficient, a landslide is defined as being induced by short-term rainfall. This splitting coefficient is not a predefined value; it is adjusted manually during the evaluation to obtain the best prediction of the rainfall threshold.

2.4. Prediction and Validation Process

We utilized landslide and rainfall databases for the period from 2014 to 2020 to create a rainfall threshold model. The model's performance was then verified using data for 2021. The entire process involved three steps (Figure 4).

- (1) Data splitting: According to the rainfall conditions, we categorized all landslides as either short-term rainfall-induced or long-term rainfall-induced. For each landslide, the short-term rainfall parameters (H1, H12, H24, and H72) and long-term rainfall parameter (D7) were calculated. Subsequently, we determined the ratios of each short-term parameter to the long-term parameter, denoted as $R1 = H1/D7$, $R12 = H12/D7$, $R24 = H24/D7$, and $R72 = H72/D7$. If the ratios for a landslide ($R1$, $R12$, $R24$, and $R72$) exceeded a specific splitting coefficient, we identified the landslide as being induced by short-term rainfall. Otherwise, it was regarded as being induced by long-term rainfall. The splitting coefficient was not a predetermined constant value but was changed in the range from 0.1 to 0.9 in the model calculations. As a result, we classified all landslides into short-term rainfall-triggered and long-term rainfall-triggered in four ways: H1–D7, H12–D7, H24–D7, and H72–D7.
- (2) Kriging interpolation: On a large scale, the short-term rainfall and long-term rainfall of each group were interpolated across the study area via Kriging using spherical variograms, which is a geostatistical technique that can be used to estimate the values of a variable at unsampled locations based on the values at sampled locations. Based on the short-term rainfall and long-term rainfall Kriging maps, we extracted the short-term rainfall values and long-term rainfall values at the exact locations of the 2021 landslide data points (Figure 4). These values served as the rainfall thresholds for 2021 landslides.

- (3) Validation: Both the long-term and short-term rainfall thresholds of 2021 landslides obtained through Kriging interpolation were compared with the actual rainfall conditions prior to landslide occurrence. A threshold larger than the actual rainfall means that our method failed to predict a landslide occurrence. Conversely, thresholds much smaller than the actual value may cause numerous false warnings. Therefore, we aimed to predict rainfall thresholds that are slightly smaller than the actual rainfall data. Hence, a successful landslide occurrence prediction was defined as the actual rainfall being within 1.0–1.5 of the calculated threshold in either the short-term condition or the long-term condition. The successful prediction rates were calculated by validating all the 2021 landslides in Dazhou using different rainfall splitting methods (Figure 4).

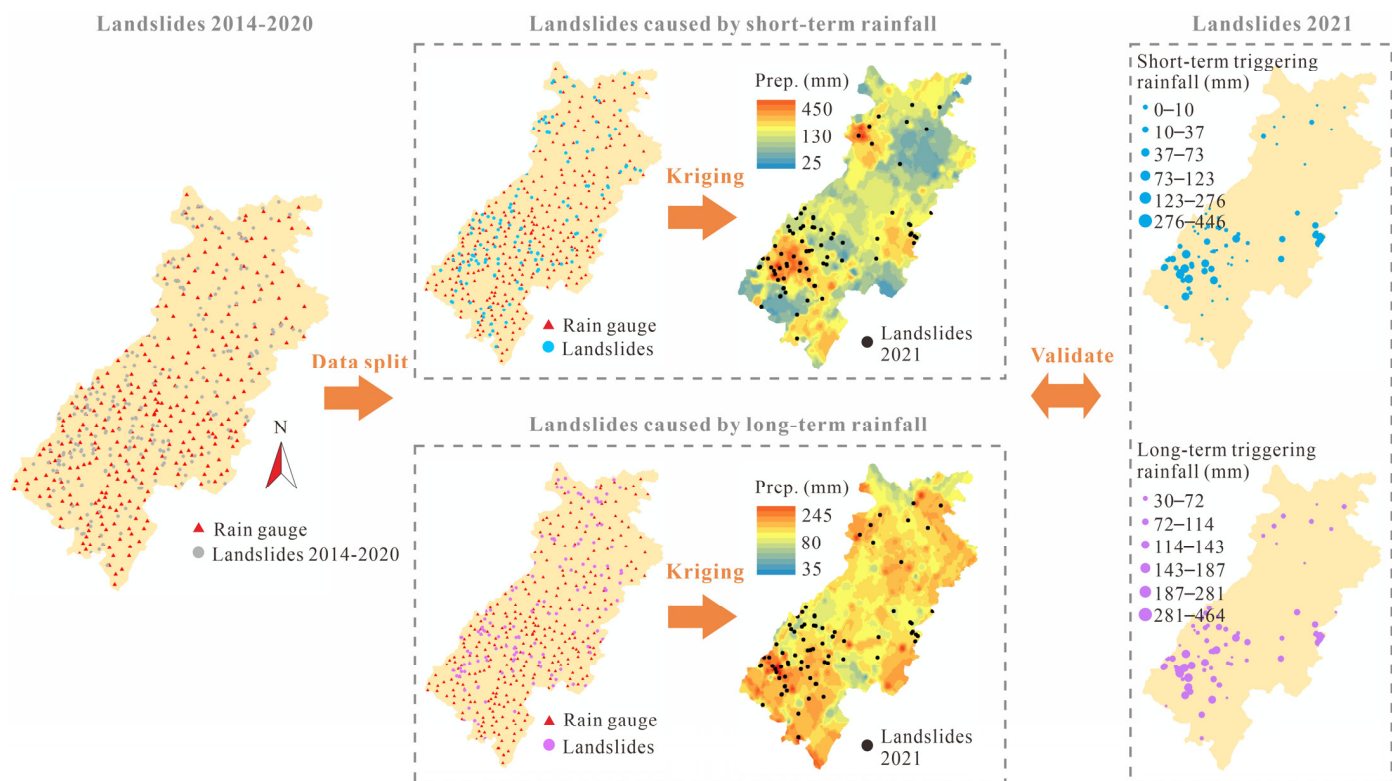


Figure 4. Workflow and general framework for the threshold method and validation process.

3. Results

3.1. Landslide-Triggering Rainfall

Figure 5 presents a comparison of the short-term rainfall and the antecedent rainfall (long-term rainfall minus short-term rainfall) for each landslide. This visual provides insights into the relationship between the two distinct rainfall conditions and the qualitative triggers associated with the landslide occurrences, namely a short-term rainfall trigger or a long-term rainfall trigger. The data points situated in close proximity to the y -axis signify a heightened probability that the landslide was prompted by short-term rainfall conditions, while those closely aligned with the x -axis denote the instances where the long-term rainfall played a decisive role. Due to the substantial gap between the 1-h rainfall and 7-day rainfall, the group H1–D7 demonstrated a majority of the data points clustering near the x -axis, indicating a prevalence of landslides triggered by long-term rainfall within this timeframe (Figure 5a). For the groups H12–D7 and H24–D7, approximately half of the landslide data are closely associated with the short-term rainfall along the y -axis, presenting a clear illustration of the influence of short-term rainfall in these scenarios (Figure 5b,c). Figure 5d reveals a concentration of data points in the vicinity of the y -axis. This observation suggests

that the rainfall occurring in the three days leading up to a landslide failure plays a more pivotal role than the overarching long-term rainfall conditions.

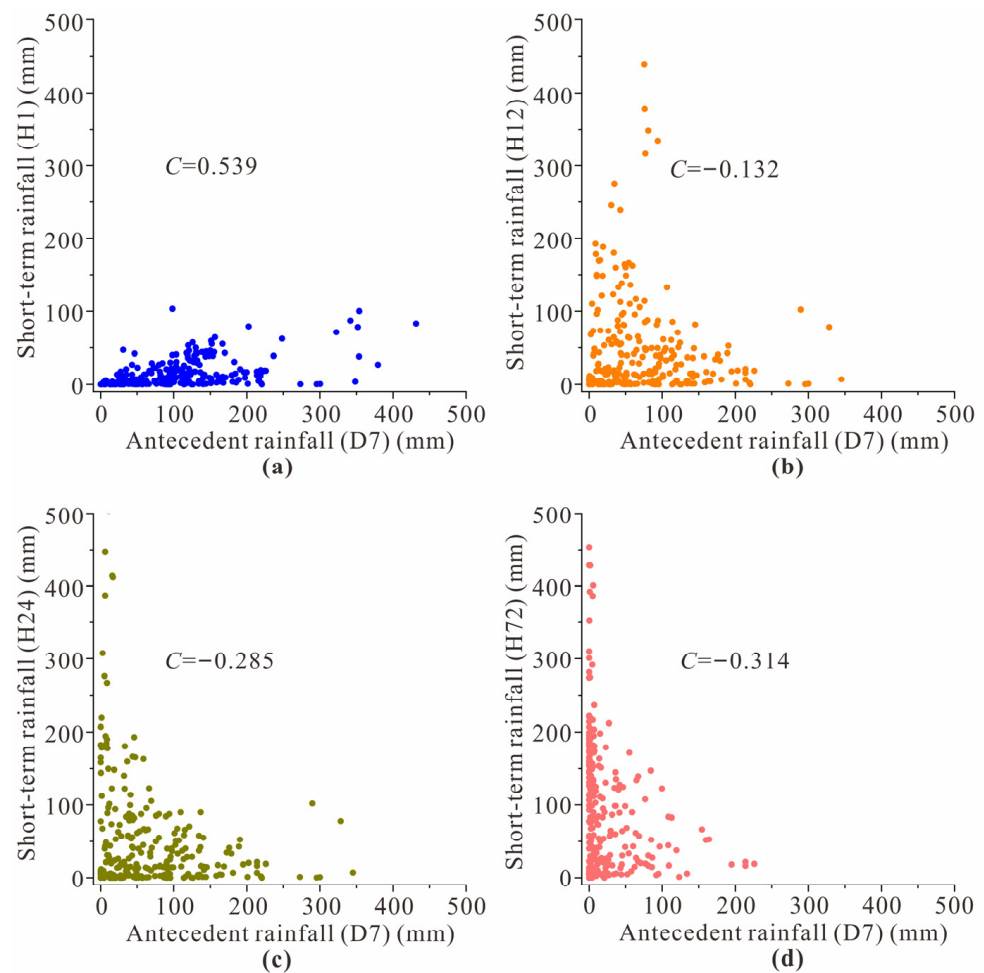


Figure 5. Short-term rainfall versus antecedent rainfall for four groups: (a) H1–D7; (b) H12–D7; (c) H24–D7; (d) H72–D7. C is the Pearson correlation coefficient.

However, the correlation map depicted in Figure 5 lacks the quantitative recognition of short-term rainfall-triggered and long-term rainfall-triggered landslides. Additionally, while the regional rainfall thresholds can be deduced from Figure 5, calculating the specific thresholds for the individual landslides remains unattainable. In general, refining the analysis by incorporating a defined splitting coefficient is crucial for the precise quantitative classification of landslides based on short-term and long-term rainfall conditions. Moreover, there is a need to develop methodologies that enable the calculation of specific rainfall thresholds for each landslide, thereby enhancing the precision of our understanding of this complex terrain.

3.2. Prediction Rates and Splitting Coefficient

The impact of different splitting coefficients on the prediction of the long-term and short-term landslides was evident, leading to varied outcomes in the prediction rates. Figure 6 provides a visual representation of this relationship for four distinct groups, H1–D7, H12–D7, H24–D7, and H72–D7. In each group, the prediction rates fluctuated in response to different coefficients. We identified the best splitting coefficient by observing the highest prediction rate depicted in Figure 6, which is pivotal for informing future practices in both long- and short-term rainfall splitting for landslide prediction.

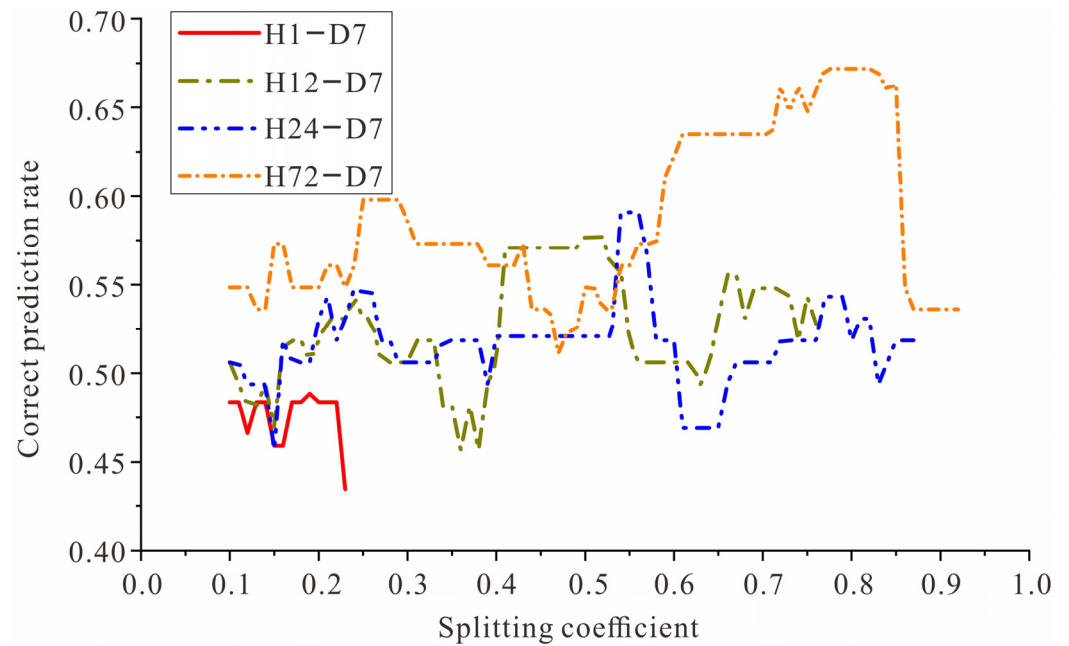


Figure 6. The relationship between the prediction rates and splitting coefficient for four short-/long-term rainfall methods.

In general, the groups with a longer short-term duration tended to yield superior predictions. The H72-D7 method exhibited relatively higher prediction rates than did the other methods. Specifically, this method achieved a commendable 67% success rate in predicting landslides when the splitting coefficient fell within the range of 0.77–0.82. In contrast, the H24-D7 and H12-D7 methods exhibited comparable results, achieving their highest prediction rates of 59% and 57%, respectively. The optimal splitting coefficients for these methods fell in the ranges of 0.54–0.56 and 0.50–0.53, respectively. On the other hand, the H1-D7 method exhibited the least favorable prediction performance, with its best splitting coefficient identified as 0.19. This resulted in the successful prediction of 48% of the landslides, indicating lower efficacy compared to the other groups. As these findings show, we not only calculated the prediction rates from the geostatistical interpolation method but also identified the most appropriate splitting coefficients.

3.3. Rainfall Threshold Distribution

Regarding the diversity in the distributions of the landslide data and thresholds, particularly at the highest prediction rate, distinct patterns unfolded among the different groups, as visually depicted in Figure 7. The short-term rainfall interpolations revealed higher thresholds in the southern region, indicating lower susceptibility to landslides under the prevailing rainfall conditions (Figure 7a,c,e). This trend was notably observed in areas like the eastern part of Da County and the middle part of Qu County. In contrast, the north of Dazhou exhibited lower thresholds, indicating a heightened risk of landslide occurrence in response to short and intense rainfall events. Notably, in specific areas of Xuanhan and Wanyuan County, rainfall surpassing 10 mm/h may act as a trigger for landslide failures (Figure 6a).

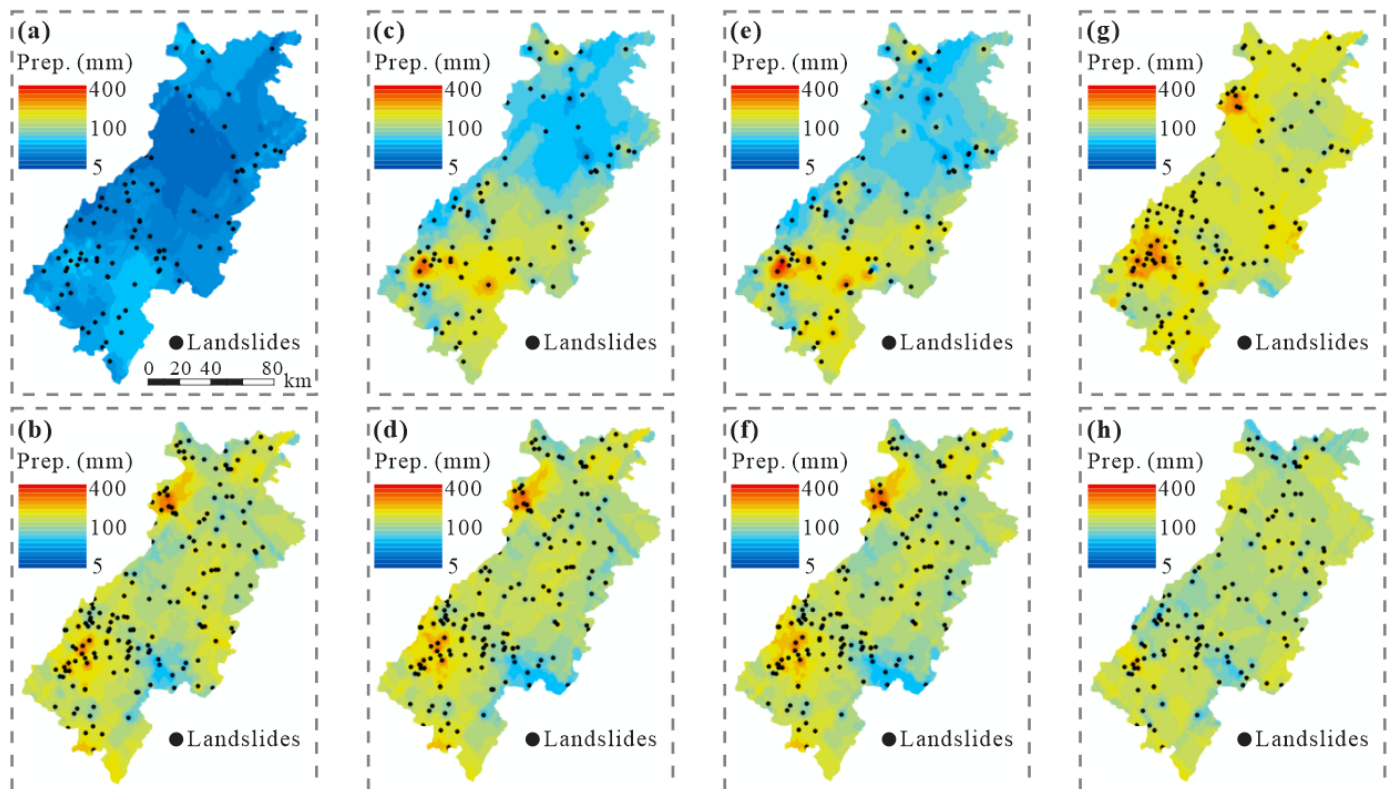


Figure 7. Landslide data points and threshold distributions in Dazhou, calculated by means of Kriging interpolation with the best splitting coefficient: (a,b) are the 1-h rainfall interpolation and 7-day rainfall interpolation from the H1–D7 prediction, respectively; (c,d) are the 12-h rainfall interpolation and 7-day rainfall interpolation from the H12–D7 prediction, respectively; (e,f) are the 24-h rainfall interpolation and 7-day rainfall interpolation from the H24–D7 prediction, respectively; (g,h) are the 72-h rainfall interpolation and 7-day rainfall interpolation from the H72–D7 prediction, respectively. The error distributions are shown in Figure S2.

On the other hand, the long-term rainfall interpolations showed a more uniform distribution, with the thresholds for most areas exceeding 200 mm in 7 days. Despite this general trend, relatively higher thresholds were observed in the central part of Qu County and the western part of Wanyuan County. Conversely, lower thresholds were found in the south of Kaijiang and Da County (Figure 7b,d,f).

In addition, the 3-day rainfall interpolation introduced a unique threshold distribution, differing from other short-term rainfall interpolations but aligning closely with the patterns observed in the long-term rainfall interpolations (Figure 7g). This observation implies that a significant proportion of landslides are triggered by rainfall accumulated over 3 days.

The distribution of the landslide points provides further insights. A substantial number of landslides are influenced by either the 3-day or long-term rainfall conditions in the northern regions of Dazhou. In contrast, in the southern regions, both the long-term and short-term rainfall conditions contribute approximately equally to the triggering of landslides.

4. Discussion

We used the Kriging interpolation method to determine the rainfall thresholds for individual landslides by simply considering the local rainfall data and the location of each landslide. Compared to the traditional experimental rainfall threshold model, this method provides the possibility of determining the rainfall threshold for each landslide location, but comparing the outputs of this method and those of the traditional empirical methods is difficult due to the differing study objectives. The traditional empirical threshold

model is based on a regional concept, focusing on regions containing various geological and geomorphological factors. Thus, susceptibility or hazard evaluations are typically performed to determine the scale of the region prior to the threshold calculation [52]. In contrast, geostatistical interpolation assumes that all the information, including the geology, geomorphology, and lithology, is dependent on a variogram-based spatial correlation between two points in space and follows a multi-Gaussian heterogeneous distribution. This approach has been widely used in climatic and geological modeling, particularly in areas where detailed data are lacking [53]. Our method is preferable as it requires minimal data for landslide susceptibility assessment, and it is also better than directly using traditional empirical models in a large region as these only consider information with a homogeneous distribution. However, this assumption is not perfect as geological and geomorphological distributions are very complex and are controlled by numerous factors. Several studies have demonstrated that the variogram-based distribution is not suitable for certain geological distributions, such as regions with highly connected formations and regions with large faults or folds [54–56]. Consequently, future research should aim to integrate more details on the geological distribution, lithological distribution, and geo-hazard distribution into geostatistical models [35].

The data quantity and quality are significant factors determining the prediction results [57]. Engineers intending to use this method must ensure the availability of a sufficient amount of landslide data and accurate rainfall gauges within the study area. The precise locations of the landslides should be obtained, and the recordings of the precipitation should be meticulous. In this study, most of the landslide data lacked the precise occurrence time in the day; the solution is using the highest precipitation value for H1 and H12. However, only 6.4% of the 78 instances for which the time was specified experienced landslide failures at the time of the highest hourly precipitation; this percentage increased to 28.2% when we extended the observation window to include the landslide occurrences within 4 h after the peak precipitation. This particular step introduced uncertainty into the subsequent predictions through Kriging interpolation. This uncertainty contributed to the lower prediction success rate observed for the H1–D7 method compared to the other techniques. Conversely, for 66.6% of the 78 instances, the landslide failures occurred within the continuous 12-h period for which the total precipitation was the largest within that day. As a result, the prediction success rate of the H12–D7 method closely aligned with that of the H24–D7 method.

Non-triggering landslide data represent another potential data-quality factor that can influence model predictions, yet this factor was not considered in this study. Accounting for the non-triggering events in the statistical analysis of a rainfall threshold significantly enhances the robustness of the threshold models [31]. In our approach, we primarily employed interpolation methods to construct the distribution of the threshold; however, the rainfall values associated with non-triggering events were omitted. This omission could lead to a higher likelihood of false alarms in the model predictions. Developing a more comprehensive method to integrate both the triggering and non-triggering events within the interpolation process presents a valuable avenue for future research. This is particularly important for areas prone to landslides with limited cases [38].

We demonstrated the performance of the geostatistical methods in predicting landslide occurrences using past rainfall information. However, in the practical applications of this method, weather forecasting is another crucial factor. Weather forecasts are more accurate in predicting the near future, such as the precipitation for the next hour, as compared to predictions for the next three days. This illustrates that the substantial errors in long-term weather forecasts may reduce the accuracy of the rainfall threshold models. Therefore, although our results revealed that the H72–D7 threshold method had the highest success rate in predicting landslides (Figure 6), H72–D7 may show the lowest prediction success rate due to the large uncertainty in the weather predictions. Therefore, potential linkages between the weather conditions and landslides are an important direction to examine in future research. Moreover, additional efforts should be undertaken to enhance the

prediction efficiency of the H1–D7 to H24–D7 models as short-term rainfall predictions are inherently more accurate in weather forecasting systems.

It is theoretically and obviously true that more landslides should occur in the northern region for the three following reasons: (i) the short-term rainfall thresholds in the north region are lower than those in the south region (Figure 7); (ii) the precipitation in the north is greater (Figure 2b); and (iii) the north region has more mountainous terrain. However, more landslides are observed in the southern region (Figure 2c). This is most likely due to the higher population and more intense human activities, such as construction and transportation infrastructure, in the southern plain area. Thus, the landslide warning and monitoring work focuses more on the southern region, resulting in more recorded landslides. Although missing data for the north do not strongly affect the thresholds if the database has enough typical data during the interpolation process, the situation implies that anthropogenic factors play a significant role in landslide prediction and monitoring. This suggests that the anthropogenic factors in the data collection and data distribution should be considered in landslide vulnerability assessments.

5. Conclusions

In this study, we systemically analyzed the hourly rainfall data from over 300 gauges and landslide data comprising 417 records from Dazhou for the period of 2014 to 2021. The landslide data were categorized into short-term rainfall-triggered landslides, based on 1-h, 12-h, 24-h, and 72-h rainfall, and long-term rainfall-triggered landslides, based on the 7-day effective rainfall, by defining a splitting coefficient. We used Kriging interpolation to extract both the long-term and short-term rainfall thresholds for each landslide in the 2014–2020 dataset. We then validated the performance of the four splitting methods using the dataset for 2021. The following conclusions were drawn:

- (1) The rainfall threshold computed by means of Kriging interpolation showed good performance in predicting the landslide occurrence in 2021. Among the four methods, the H72–D7 threshold model yielded the best prediction rate of 67%. H1–D7, H12–D7, and H24–D7 showed correct prediction rates of 48%, 57%, and 59%, respectively. This is contrary to weather forecasting, in which the rainfall predictions of the near future demonstrated better performance. Therefore, the application of geostatistical methods may need to consider the accuracy of weather forecasts.
- (2) Through the best prediction rate, we quantitatively determined the best splitting coefficients to divide the landslides into short-term rainfall-triggered and long-term rainfall-triggered events. The best splitting coefficients for H1/D7, H12/D7, H24/D7, and H72/D7 were 0.19, 0.50–0.53, 0.54–0.56, and 0.77–0.82, respectively. These coefficients can be used in future landslide analyses to improve the landslide warning system.
- (3) Multiple factors may impact the accuracy of a rainfall threshold model, such as the landslide distribution, weather forecasts, and anthropogenically influenced recordings. A more comprehensive empirical model represents a promising avenue for future research.

Supplementary Materials: The following supporting information can be downloaded at <https://www.mdpi.com/article/10.3390/su16104044/s1>, Figure S1: The distribution of landslide data with exact occurrence time; Figure S2: Standard deviations (Std) of Kriging interpolation in Figure 7.

Author Contributions: Conceptualization, Z.X. (Zhongyuan Xu), Z.X. (Zhilin Xiao) and Z.M.; methodology, Z.X. (Zhongyuan Xu) and Q.Z.; software, Z.X. (Zhongyuan Xu); validation, Z.X. (Zhilin Xiao), X.Z. (Xiaoyan Zhao) and P.Z.; formal analysis, Z.X. (Zhongyuan Xu); investigation, Z.X. (Zhongyuan Xu); resources, P.Z. and X.Z. (Xiaoqiong Zhang); data curation, Z.X. (Zhilin Xiao), P.Z. and X.Z. (Xiaoqiong Zhang); writing—original draft preparation, Z.X. (Zhongyuan Xu); writing—review and editing, Z.X. (Zhilin Xiao), X.Z. (Xiaoyan Zhao) and Z.M.; visualization, Z.X. (Zhongyuan Xu); supervision, Z.X. (Zhilin Xiao) and X.Z. (Xiaoyan Zhao); project administration, Z.X. (Zhilin Xiao); funding

acquisition, Z.X. (Zhongyuan Xu) and Z.M. All authors have read and agreed to the published version of the manuscript.

Funding: This research was funded by Natural Science Foundation of Sichuan Province, grant number 2023NSFSC0788; Fundamental Research Funds for the Central Universities, grant number 2682022KJ055; Research funds from Sichuan Institute of Land and Space Ecological Restoration and Geological Hazard Prevention, grant number SXFY-KJ-2022-01; Research Project of Geologic Hazards Early Warning Model and Threshold in Lu Shan Earthquake Disaster Area, grant number N5118012023000092.

Institutional Review Board Statement: Not applicable.

Informed Consent Statement: Not applicable.

Data Availability Statement: Data are available upon reasonable request.

Acknowledgments: The authors sincerely appreciate the precipitation data supply from the Sichuan Provincial Meteorological Service.

Conflicts of Interest: The authors declare no conflicts of interest.

References

1. Aleotti, P.; Chowdhury, R. Landslide hazard assessment: Summary review and new perspectives. *Bull. Eng. Geol. Environ.* **1999**, *58*, 21–44. [\[CrossRef\]](#)
2. Yao, W.M.; Li, C.D.; Zhan, H.B.; Zeng, J.B. Time-dependent slope stability during intense rainfall with stratified soil water content. *Bull. Eng. Geol. Environ.* **2019**, *78*, 4805–4819. [\[CrossRef\]](#)
3. Yu, P.; Liu, H.; Yu, H.; Xie, Y.; Yu, Y.; Zhu, C.; Dong, J.; Guang, Y. Study on fluid–solid coupling numerical simulation and early warning of weathered granite landslides induced by extreme rainfall. *Sustainability* **2023**, *15*, 11738. [\[CrossRef\]](#)
4. Baum, R.L.; Godt, J.W. Early warning of rainfall-induced shallow landslides and debris flows in the USA. *Landslides* **2010**, *7*, 259–272. [\[CrossRef\]](#)
5. Offenthaler, I.; Felderer, A.; Formayer, H.; Glas, N.; Leidinger, D.; Leopold, P.; Schmidt, A.; Lexer, M.J. Threshold or limit? precipitation dependency of Austrian landslides, an ongoing challenge for hazard mapping under climate change. *Sustainability* **2020**, *12*, 6182. [\[CrossRef\]](#)
6. Segoni, S.; Lagomarsino, D.; Fanti, R.; Moretti, S.; Casagli, N. Integration of rainfall thresholds and susceptibility maps in the Emilia Romagna (Italy) regional-scale landslide warning system. *Landslides* **2015**, *12*, 773–785. [\[CrossRef\]](#)
7. Maurizio, L.; Maria, D. A multiple temporal kernel density estimation approach for new triggered landslides forecasting and susceptibility assessment. *Disaster Adv.* **2012**, *5*, 100–108.
8. Guzzetti, F.; Peruccacci, S.; Rossi, M.; Stark, C.P. Rainfall thresholds for the initiation of landslides in central and southern Europe. *Meteorol. Atmos. Phys.* **2007**, *98*, 239–267. [\[CrossRef\]](#)
9. Marin, R.J. Physically based and distributed rainfall intensity and duration thresholds for shallow landslides. *Landslides* **2020**, *17*, 2907–2917. [\[CrossRef\]](#)
10. Sheng, Y.; Li, Y.; Xi, G.; Li, Z. Threshold assessment of rainfall-induced landslides in Sangzhi County: Statistical analysis and physical model. *Bull. Eng. Geol. Environ.* **2022**, *81*, 388. [\[CrossRef\]](#)
11. Segoni, S.; Piciullo, L.; Gariano, S.L. A review of the recent literature on rainfall thresholds for landslide occurrence. *Landslides* **2018**, *15*, 1483–1501. [\[CrossRef\]](#)
12. Lazzari, M.; Piccarreta, M.; Capolongo, D. Landslide triggering and local rainfall thresholds in Bradanic Foredeep, Basilicata region (Southern Italy). In *Landslide Science and Practice*; Margottini, C., Canuti, P., Sassa, K., Eds.; Springer: Rome, Italy, 2013; Volume 2, pp. 671–677.
13. Rosi, A.; Peternel, T.; Jemec-Auflič, M.; Komac, M.; Segoni, S.; Casagli, N. Rainfall thresholds for rainfall-induced landslides in Slovenia. *Landslides* **2016**, *13*, 1571–1577. [\[CrossRef\]](#)
14. Zhang, S.; Xu, C.; Wei, F.; Hu, K.; Xu, H.; Zhao, L.; Zhang, G. A physics-based model to derive rainfall intensity-duration threshold for debris flow. *Geomorphology* **2020**, *351*, 106930. [\[CrossRef\]](#)
15. Guo, X.; Cui, P.; Li, Y. Debris flow warning threshold based on antecedent rainfall: A case study in Jiangjia Ravine, Yunnan, China. *J. Mt. Sci. Engl.* **2013**, *10*, 305–314. [\[CrossRef\]](#)
16. Yang, H.; Wei, F.; Ma, Z.; Guo, H.; Su, P.; Zhang, S. Rainfall threshold for landslide activity in Dazhou, southwest China. *Landslides* **2020**, *17*, 61–77. [\[CrossRef\]](#)
17. Aleotti, P. A warning system for rainfall-induced shallow failures. *Eng. Geol.* **2004**, *73*, 247–265. [\[CrossRef\]](#)
18. Peruccacci, S.; Brunetti, M.T.; Gariano, S.L.; Melillo, M.; Rossi, M.; Guzzetti, F. Rainfall thresholds for possible landslide occurrence in Italy. *Geomorphology* **2017**, *290*, 39–57. [\[CrossRef\]](#)
19. Hong, Y.; Hiura, H.; Shino, K.; Suemine, A.; Fukuoka, H.; Wang, G. The influence of intense rainfall on the activity of large-scale crystalline schist landslides in Shikoku Island, Japan. *Landslides* **2005**, *2*, 97–105. [\[CrossRef\]](#)

20. Liu, S.; Wei, L.; Hu, K. Topographical and geological variation of effective rainfall for debris-flow occurrence from a large-scale perspective. *Geomorphology* **2020**, *358*, 107134. [[CrossRef](#)]
21. Martelloni, G.; Segoni, S.; Fanti, R.; Catani, F. Rainfall thresholds for the forecasting of landslide occurrence at regional scale. *Landslides* **2012**, *9*, 485–495. [[CrossRef](#)]
22. Guzzetti, F.; Gariano, S.L.; Peruccacci, S.; Brunetti, M.T.; Marchesini, I.; Rossi, M.; Melillo, M. Geographical landslide early warning systems. *Earth Sci. Rev.* **2020**, *200*, 102973. [[CrossRef](#)]
23. Crosta, G.B.; Frattini, P. Rainfall thresholds for triggering soil slips and debris flow. In Proceedings of the 2nd EGS Plinius Conference, Siena, Italy, 1–3 October 2001.
24. Cannon, S.H.; Gartner, J.E. Wildfire-related debris flow from a hazards perspective. In *Debris Flow Hazards and Related Phenomena*; Jakob, M., Hungr, O., Eds.; Springer: Berlin/Heidelberg, Germany, 2005; pp. 363–385.
25. Miller, S.; Brewer, T.; Harris, N. Rainfall thresholding and susceptibility assessment of rainfall-induced landslides: Application to landslide management in St Thomas, Jamaica. *Bull. Eng. Geol. Environ.* **2009**, *68*, 539–550. [[CrossRef](#)]
26. Monsiers, E.; Dewitte, O.; Demoulin, A. A susceptibility-based rainfall threshold approach for landslide occurrence. *Nat. Hazards Earth Syst. Sci.* **2019**, *19*, 775–789. [[CrossRef](#)]
27. Marin, R.J.; García, E.F.; Aristizábal, E. Effect of basin morphometric parameters on physically-based rainfall thresholds for shallow landslides. *Eng. Geol.* **2020**, *278*, 105855. [[CrossRef](#)]
28. Abraham, M.T.; Satyam, N.; Rosi, A.; Pradhan, B.; Segoni, S. The selection of rain gauges and rainfall parameters in estimating intensity-duration thresholds for landslide occurrence: Case study from wayanad (India). *Water* **2020**, *12*, 1000. [[CrossRef](#)]
29. Al-Thwaynee, O.F.; Melillo, M.; Gariano, S.L.; Park, H.J.; Kim, S.; Lombardo, L.; Hafer, P.; Mohajane, M.; Quevedo, R.P.; Catani, F.; et al. DEWS: A QGIS tool pack for the automatic selection of reference rain gauges for landslide-triggering rainfall thresholds. *Environ. Modell. Softw.* **2023**, *162*, 105657. [[CrossRef](#)]
30. Gariano, S.L.; Melillo, M.; Peruccacci, S.; Brunetti, M.T. How much does the rainfall temporal resolution affect rainfall thresholds for landslide triggering? *Nat. Hazards* **2020**, *100*, 655–670. [[CrossRef](#)]
31. Leonarduzzi, E.; Molnar, P. Deriving rainfall thresholds for landsliding at the regional scale: Daily and hourly resolutions, normalisation, and antecedent rainfall. *Nat. Hazards Earth Syst. Sci.* **2020**, *20*, 2905–2929. [[CrossRef](#)]
32. Zhao, B.; Dai, Q.; Han, D.; Zhang, J.; Zhuo, L.; Berti, M. Application of hydrological model simulations in landslide predictions. *Landslides* **2020**, *17*, 877–891. [[CrossRef](#)]
33. Zhuang, J.; Peng, J.; Wang, G.; Iqbal, J.; Wang, Y.; Li, W.; Xu, Q.; Zhu, X. Prediction of rainfall-induced shallow landslides in the Loess Plateau, Yan'an, China, using the TRIGRS model. *Earth Surf. Proc. Land.* **2016**, *42*, 915–927. [[CrossRef](#)]
34. Gariano, S.L.; Brunetti, M.T.; Iovine, G.; Melillo, M.; Peruccacci, S.; Terranova, O.; Vennari, C.; Guzzetti, F. Calibration and validation of rainfall thresholds for shallow landslide forecasting in Sicily, southern Italy. *Geomorphology* **2015**, *228*, 653–665. [[CrossRef](#)]
35. Vessia, G.; Curzio, D.D.; Chiaudani, A.; Rusi, S. Regional rainfall threshold maps drawn through multivariate geostatistical techniques for shallow landslide hazard zonation. *Sci. Total. Environ.* **2020**, *705*, 135815. [[CrossRef](#)]
36. Xu, Q.; Zeng, Y.; Qian, J.; Wang, C.; He, C. Study on an improved tangential angle and the corresponding landslide pre-warning criteria. *Geol. B. Chin.* **2009**, *28*, 501–505.
37. Steger, S.; Moreno, M.; Crespi, A.; Zellner, P.J.; Gariano, S.L.; Brunetti, M.T.; Melillo, M.; Peruccacci, S.; Marra, F.; Kohrs, R.; et al. Deciphering seasonal effects of triggering and preparatory precipitation for improved shallow landslide prediction using generalized additive mixed models. *Nat. Hazards Earth Syst. Sci.* **2023**, *23*, 1483–1506. [[CrossRef](#)]
38. Peres, D.J.; Cancelliere, A. Comparing methods for determining landslide early warning thresholds: Potential use of non-triggering rainfall for locations with scarce landslide data availability. *Landslides* **2021**, *18*, 3135–3147. [[CrossRef](#)]
39. Gonzalez, F.C.G.; Cavacanti, M.C.R.; Ribeiro, W.N.; de Mendonça, M.B.; Haddad, A.N. A systematic review on rainfall thresholds for landslides occurrence. *Heliyon* **2024**, *10*, e23247. [[CrossRef](#)]
40. Montrasio, L.; Valentino, R.; Losi, G.L. Towards a real-time susceptibility assessment of rainfall-induced shallow landslides on a regional scale. *Nat. Hazards Earth Syst. Sci.* **2011**, *11*, 1927. [[CrossRef](#)]
41. Zhang, M.; Liu, J. Controlling factors of loess landslides in western China. *Environ. Earth Sci.* **2009**, *59*, 1671–1680. [[CrossRef](#)]
42. Bonnard, C.H.; Noverraz, F. Influence of climate change on large landslides: Assessment of long-term movements and trends. In Proceedings of the International Conference on Landslides: Causes Impact and Countermeasures, Davos, Switzerland, 17–21 June 2001.
43. Crosta, G.B. Regionalization of rainfall thresholds: An aid to landslide hazard evaluation. *Environ. Geol.* **1998**, *35*, 131–145. [[CrossRef](#)]
44. Liu, L.; Zhou, L.; Ao, T.; Liu, X.; Shu, X. Flood hazard analysis based on rainfall fusion: A case study in Dazhou City, China. *Remote Sens.* **2022**, *14*, 4843. [[CrossRef](#)]
45. Carpenter, C. Sichuan Basin Evergreen Broadleaf Forests. Available online: <https://www.oneearth.org/ecoregions/sichuan-basin-evergreen-broadleaf-forests/> (accessed on 7 February 2024).
46. Yang, Y.; Wen, L.; Luo, B.; Song, J.; Chen, X.; Wang, X.; Hong, H.; Zhou, G.; He, Q.; Zhang, X.; et al. Sedimentary tectonic evolution and reservoir-forming conditions of the Dazhou–Kaijiang paleo-uplift, Sichuan Basin. *Nat. Gas Ind. B* **2016**, *3*, 515–525. [[CrossRef](#)]

47. Marin, R.J.; Velásquez, M.F.; García, E.F.; Alvioli, M.; Aristizábal, E. Assessing two methods of defining rainfall intensity and duration thresholds for shallow landslides in data-scarce catchments of the Colombian Andean Mountains. *Catena* **2021**, *206*, 105563. [[CrossRef](#)]
48. Bruce, J.P.; Clark, R.H. *Introduction to Hydrometeorology*; Pergamon: Oxford, UK, 1966.
49. Ran, P.; Li, S.; Zhou, G.; Wang, X.; Meng, M.; Liu, L.; Chen, Y.; Huang, H.; Ye, Y.; Lei, X. Early identification and influencing factors analysis of active landslides in mountainous areas of Southwest China using SBAS–InSAR. *Sustainability* **2023**, *15*, 4366. [[CrossRef](#)]
50. Guzzetti, F.; Peruccacci, S.; Rossi, M.; Stark, C.P. The rainfall intensity-duration control of shallow landslides and debris flows: An update. *Landslides* **2008**, *5*, 3–17. [[CrossRef](#)]
51. Zhuang, J.; Javed, I.; Peng, J.; Liu, T. Probability Prediction Model for Landslide Occurrences in Xi'an, Shaanxi Province, China. *J. Mt. Sci. Engl.* **2014**, *11*, 345–359. [[CrossRef](#)]
52. Hsu, C.F. Rainfall-induced landslide susceptibility assessment and the establishment of early warning techniques at regional scale. *Sustainability* **2023**, *15*, 16764. [[CrossRef](#)]
53. Pyrcz, M.J.; Deutsch, C.V. *Geostatistical Reservoir Modeling*, 2nd ed.; Oxford University Press: Oxford, UK, 2014.
54. Liu, A.; Zheng, L.; Deng, J.; Huang, Y. Landslide susceptibility of the Xiangjiaba Reservoir area associated with the Yaziba Fault. *Bull. Eng. Geol. Environ.* **2017**, *77*, 1–11. [[CrossRef](#)]
55. Xu, Z.; Hu, B.X.; Xu, Z.; Wu, X. Numerical study of groundwater flow cycling controlled by seawater/freshwater interaction in Woodville Karst Plain. *J. Hydrol.* **2019**, *579*, 124171. [[CrossRef](#)]
56. Xu, Z.; Khan, M.R.; Ahmed, K.M.; Zahid, A.; Hariharan, J.; Passalacqua, P.; Steel, E.; Chadwick, A.; Paola, C.; Goofbred, S.L.; et al. Predicting subsurface architecture from surface channel networks in the Bengal Delta. *J. Geophys. Res. Earth* **2023**, *128*, e2022JF006775. [[CrossRef](#)]
57. Peruccacci, S.; Gariano, S.L.; Melillo, M.; Solimano, M.; Guzzetti, F.; Brunetti, M.T. The ITALian rainfall-induced Landslides CAtalogue, an extensive and accurate spatio-temporal catalogue of rainfall-induced landslides in Italy. *Earth Syst. Sci. Data* **2023**, *15*, 2863–2877. [[CrossRef](#)]

Disclaimer/Publisher’s Note: The statements, opinions and data contained in all publications are solely those of the individual author(s) and contributor(s) and not of MDPI and/or the editor(s). MDPI and/or the editor(s) disclaim responsibility for any injury to people or property resulting from any ideas, methods, instructions or products referred to in the content.